front of the DCSW and, hence, $\Delta\tilde{E}$ are appreciably greater. This also leads to the intensive development of cavitational flow.

In accordance with the experimental results obtained here, a reduction in τ (i.e., a reduction in the time of propagation of the SW) is accompanied by a reduction in the energy threshold for failure of the fluid volume. Thus, with a decrease in $\bar{\tau}$ from 9.4 to 2.26, the value of e_* decreases from 5 to 1.3 J/g. This is evidently connected with the fact that at $\bar{\tau} = 2.26$, nearly all of the energy of the DCSW is converted to work to expand cavitation bubbles, while at $\bar{\tau} = 9.4$ it is converted to kinetic energy associated with the radial expansion of the fluid ring. Only part of this energy is expended on the development of perturbations on the boundaries of the fluid volume, which also lead to its failure.

If we introduce the parameter $N = e/\tau$ — the rate of release of explosive energy (i.e., the rate of release of specific explosive energy averaged over the loading time), then at $e = e_*$ the parameter $N_* = e_*/\tau$ takes similar values in all of the cases shown in Fig. 2b-d: $N_* = 40$, 36, and 43 kJ/(g·sec), respectively. Thus, whereas e_* depends on the loading time (i.e., on the parameters of the SW and the explosion bubble), the threshold value of the rate of release of explosive energy N_* is a more universal parameter. It characterizes the energy threshold for failure of the water volume, since loading remains nearly constant within the range of conditions examined here.

We thank V. K. Kendrinskii for his discussion of this investigation.

LITERATURE CITED

1. S. V. Stebnovskii and N. N. Chernobaev, "Energy threshold in the impulsive failure of a fluid volume," Zh. Prikl. Mekh. Tekh. Fiz., No. 1 (1986).
2. S. V. Stebnovskii, "Stability of the free boundaries of a fluid piston moving with acceleration in an axisymmetric channel," Din. Sploshn. Sredy, 15 (1973).
3. B. V. Zamyshlayev and Yu. S. Yakovlev, Dynamic Loads in an Underwater Explosion [in Russian], Sudostroenie, Leningrad (1967).
4. V. K. Kedrinskii, "Surface effects in an underwater explosion (survey)," Zh. Prikl. Mekh. Tekh. Fiz., No. 4 (1978).

CALCULATION OF THE DISPERSION OF A COMPRESSED VOLUME OF A GAS SUSPENSION

Yu. V. Kazakov, A. V. Fedorov, and V. M. Fomin

UDC 532.529:533.6.071.1

Much attention is currently being given to the physical and mathematical modeling of multiphase systems due to the extensive use of various types of technologies which involve heterogeneous and homogeneous media. Surveys of the mathematical modeling of certain problems of the mechanics of heterogeneous media can be found in [1-3].

In experiments set up to study the wave dynamics of a gas suspension of solid particles, the emphasis is generally placed on the interaction of shock waves (SW) with clouds of dust-laden gas. An experimental study was made in [4] of the rarefaction of a gas suspension in order to examine the effect of the dust content of a medium with a high mass content of particles under high pressure on the parameters of a shock wave formed in the discharge of such a medium into free space. The question of the discharge conditions is important from the viewpoint of the safety of different types of equipment (pipelines for transporting bulk materials, chemical reactors employing fluidization, etc.). The process of rarefaction of a gas suspension was examined in [5]. Here, the authors ignored the volume content of particles and analyzed the dispersion of a gas suspension in a vacuum. The study [6] calculated the explosive dispersion of a cloud of a gas suspension in the case of relatively small volume contents of the disperse phase, while the study [7] examined an outburst of coal and

Novosibirsk. Translated from Zhurnal Prikladnoi Mekhaniki i Tekhnicheskoi Fiziki, No. 5, pp. 139-144, September-October, 1987. Original article submitted April 7, 1986.

0021-8944/87/2805-0773$12.50

gas in an equilibrium approximation. A more complete bibliography of the experimental and theoretical investigations of the dynamics of gas suspensions can be found in [1-3, 8].

We will examine the solution of the problem of determining the flow in a shock tube in the case where the high-pressure chamber (HPC) of the tube contains a gas suspension of fine particles and the low-pressure chamber (LPC) contains air (GP problem). The mixture is separated from the gas by a diaphragm which ruptures at the initial moment of time. This allows a shock wave (SW) to propagate into the low-pressure region. The wave is followed in succession by a contact discontinuity and a combination discontinuity (CBD). A rarefaction wave (RW) propagates in the gas suspension. After the RW is reflected from the wall of the HPC, when the RW and SW begin to interact, the SW undergoes attenuation. We will also study the G problem — the variant of the GP problem when the HPC contains pure gas.

It was established in [4] that compared to the case of pure gas in the HPC, the amplitude of the resulting shock waves is low and it takes longer for the formation of a triangular pressure pulse. It is also apparent that the process in question cannot be described within the framework of an equilibrium approach. In fact, the simplest analysis of the characteristic times [9] for the process studied in [4] shows that at $d \gtrsim 10$ μm the characteristic duration of the gas-dynamic process is less than the velocity and temperature relaxation times. This is due to the nonequilibrium of the process. Thus, here we analyzed the process of rarefaction of a gas suspension within the framework of nonequilibrium theory for large-volume fractions of the disperse phase.

The equations describing this flow in a nonequilibrium approximation have the form

$$\partial\rho_i/\partial t + \partial\rho_i u_i/\partial x = 0,$$
$$\partial\rho_i u_i/\partial t + \partial\rho_i u_i^2/\partial x + m_i\partial p/\partial x = (-1)^{i+1} f,$$
$$\partial(\rho_1 E_1 + \rho_2 E_2)/\partial t + \partial(\rho_1 u_1 E_1 + \rho_2 u_2 E_2 + p(m_1 u_1 +$$
$$+ m_2 u_2))/\partial x = 0,\ \partial\rho_2 e_2/\partial t + \partial\rho_2 u_2 e_2/\partial x = q,$$
$$p = \rho_{11} R T_1,\ m_1 + m_2 = 1,\ \rho_i = \rho_{ii} m_i,\ \rho_{22} = \text{const},$$
$$e_i = c_i T_i,\ E_i = e_i + u_i^2/2,\ i = 1, 2.$$

Here ρ_i, u_i, e_i, T_i, m_i are the mean density, velocity, internal energy, temperature, and volume fraction of the i-th phase (the subscript i = 1 pertains to parameters of the gas, i = 2 pertains to parameters of the particles); p is pressure; E_i is the total energy of the i-th phase; the terms f and q, describing the mechanical and thermal interaction of the phases, are analogous to those used in [10]:

$$f = 0{,}125 n\pi d^2 C_D \rho_{11}|u_1 - u_2|(u_1 - u_2),\ n = 6m_2/\pi d^3,$$
$$C_D = \begin{cases} C_1 = 24/\mathrm{Re} + 4{,}4/\mathrm{Re}^{0,5} + 0{,}42, & m_2 \leqslant 0{,}08, \\ C_2 = (4/3\, m_1)(1{,}75 + 150\,(m_1\mathrm{Re})^{-1}), & m_2 > 0{,}45, \\ ((m_2 - 0{,}08)\, C_2 + (0{,}45 - m_2)\, C_1)/0{,}35, & 0{,}08 < m_2 \leqslant 0{,}45, \end{cases}$$
$$q = n\pi d\lambda\, \mathrm{Nu}\,(T_1 - T_2),$$
$$\mathrm{Nu} = \begin{cases} 2 + 0{,}106\mathrm{Re}\mathrm{Pr}^{0,33}, & \mathrm{Re} \leqslant 200, \\ 2{,}274 + 0{,}6\mathrm{Re}^{0,67}\mathrm{Pr}^{0,33}, & \mathrm{Re} > 200, \end{cases}$$
$$\mathrm{Re} = \rho_{11}|u_1 - u_2|d/\mu,\ \mathrm{Pr} = c_2\lambda/\mu.$$

The above system of equations was solved with the following initial-boundary conditions and parameter values: $0 < x < \ell_0 = 0.07$ m: $m_1 = 0.8375$, $m_2 = 0.1625$, $u_1 = u_2 = 0$, $\eta = \rho_2/\rho_1 = 50$, $T_1 = T_2 = 300$ K, $\rho_{11} = 5.651$ kg/m³, $\rho_{22} = 1460$ kg/m³, $\gamma = 1.66$, $c_2 = 710$ m²/(sec·deg), $c_1 = 3128$ m²/(sec²·deg), $\mu = 1.85 \cdot 10^{-5}$ kg/(m·sec), $\lambda = 0.143$ kg·m/(sec³/deg); $x \leq 0$: $m_1 = 1$, $m_2 = 0$, $u_1 = 0$, $T_1 = 300$ K, $\gamma = 1.4$, $c_1 = 716$ m²/(sec²·deg), $\rho_{11} = 0.11639\text{-}11.639$ kg/m³; $x = \ell_0$: $u_1(t) = 0$.

To perform the calculations, we used a modification of the coarse particle method, with tracking of the contact and combination discontinuities [6]. This algorithm has been previously tested only for exact solutions of gas-dynamic equations [11]. It is useful to perform test calculations for exact solutions of equations of the mechanics of heterogeneous media as well [8]. This topic is even more fundamental, since it is known that the system of equations is nonhyperbolic in the case of velocity nonequilibrium with $(u_1 - u_2)^2 < a^2(1 + (\rho_{11}m_2/\rho_{22}m_1)^{1/3})^3$ [8, 12, 13]. The problem of the stability of difference methods

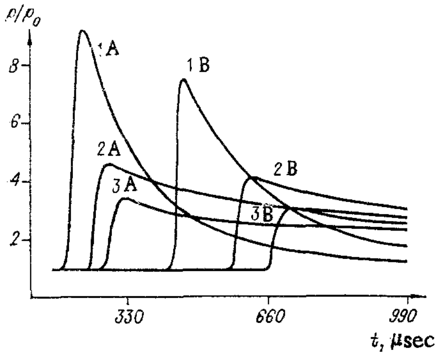

Fig. 1

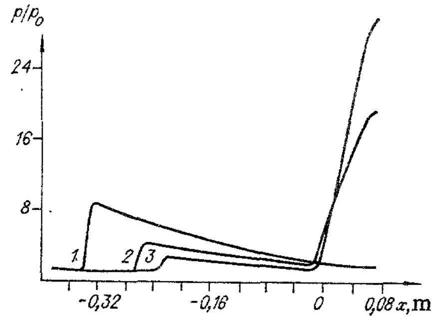

Fig. 2

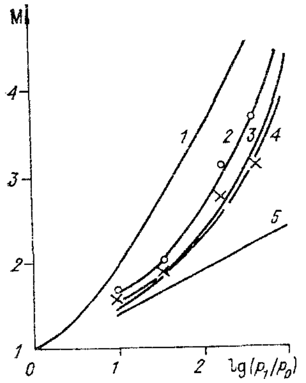

Fig. 3

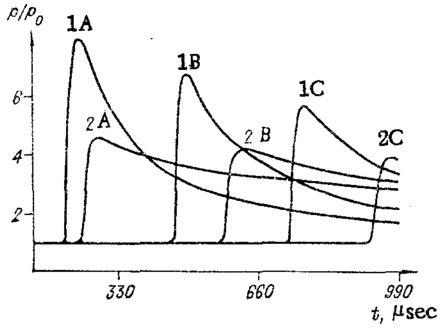

Fig. 4

for two-velocity models was discussed in [13, 14], where it was noted that at $h \gg d$ (h is the mesh of the difference grid and d is the diameter of an occlusion of the disperse phase) the characteristic buildup period of perturbations (with a wavelength ~ h) which can be generated in the computation is significantly greater than the characteristic relaxation time. Thus, on the given difference grid, perturbations will not build up for a certain relationship between τ and h which follows from the Curant condition. Here, it is natural to require that $h \gg d$, since we are using a continuum approach to describe particles of a gas suspension, and effects with a characteristic size d cannot be described in this case. As a test calculation, we solved the problem of the propagation of a steady isothermal shock wave in a gas suspension [8]. It was found that the difference solution is close to the analytical solution, the discontinuity becomes diffuse over 4-5 cells of the grid, and the relaxation zone is satisfactorily reproduced. The test calculation allowed us to analyze certain features of the numerical investigation of problems of the mechanics of heterogeneous media.

Let us proceed to the discussion the results of calculations of the above-formulated problem. Figure 1 shows pressure distributions over time: A) at the point $x = -0.2$ m, B) at the point $x = -0.44$ m, 1) problem G, 2) problem GP, $\eta = 50$, $d = 100$ μm, 3) $\eta = 50$, $d = 20$ μm at $p_1/p_0 = 35$. It is evident that in the G case, a characteristic triangular profile has already been formed. This contrasts with the case GP, where flow is represented by a nearly stepped pulse with a shock wave of lower amplitude. Figure 2 shows pressure distributions in the tube at the moment of time t = 330 sec. Here, 1 corresponds to the problem G, and 2 and 3 correspond to the problem GP at $\eta = 50$ and $d = 100$ and 20 μm, respectively. It is evident that gas pressure in the HPC decreases more rapidly in problem G than in problem GP, which is due to interphase friction and heat transfer. The characteristic pressure decay time in the HPC increases with a decrease in particle diameter for a fixed mass ratio η. A reduction in particle diameter leads to an increase in the drag which the particles exert on the gas and to more intensive entrainment of particles. The latter is a consequence of the fact that the expression for the resistance force contains terms which are proportional to d^{-1} and d^{-2}. Heat transfer also intensifies with a reduction in particle diameter. On the one hand, the gas is cooled as the RW passes. On the other hand, it is heated due to presence of warm particles.

The results of the calculations were used to construct the dependence of the mean velocity of the SW on the section between $x = -0.2$ m and $x = -0.68$ m on the initial ratio of

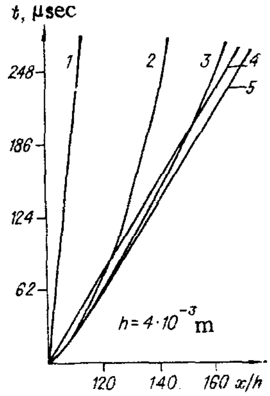

Fig. 5

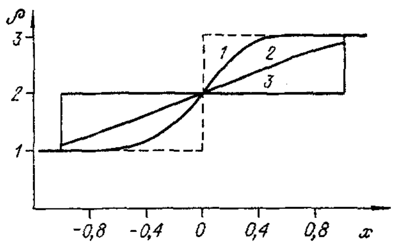

Fig. 6

pressures on the diaphragm with a fixed pressure in the HPC. It should be noted that the velocity is variable in this case, since the RW reflected from the wall catches up with the SW, and the SW is slowed as a result of its interaction with the RW. This fact was not specified in [4], although it is obvious that it might be important in certain situations. Figure 3 shows theoretical dependences of the Mach number of the SW on log (p_1/p_0): 2) $\eta = 50$, $d = 100$ μm, 4) $\eta = 50$, $d = 20$ μm; 3) experiment, 1) G Flow, 5) theoretical curve obtained within the framework of the equilibrium approach. It can be seen that the dependence of the velocity of the SW on log (p_1/p_0) for nonequilibrium flow lies within the boundaries corresponding to frozen and equilibrium flow [4]. The study [4] did not report any information on the size of the particles used in the experiment. However, it can be seen from Fig. 3 that the most satisfactory agreement between the theoretical and experimental curve is obtained at $d = 20$ μm. This makes it possible to assume that particles with an effective diameter $d = 20$ μm were used in the experiment. The accuracy of this conclusion is on the same order as the accuracy of our representation of the parameters characterizing the mechanical and thermal interaction of the phases. Figure 4 shows distributions of gas pressure at $\eta = 50$, $d = 100$ μm, and $p_1/p_0 = 35$ at points A ($x = -0.2$ m), B ($x = -0.44$), and C($x = -0.68$ m). Here, 1 shows values for C_D and Nu from [10], while 2 shows values for $c_D = 24/\mathrm{Re}$ and $\mathrm{Nu} = 2$. The second variant of description of the phase interaction leads to a situation whereby the mechanical and thermal interaction of the phases is reduced considerably and the flow approximates frozen flow.

Let us deal briefly with the structure of the RW in the gas suspension next to the quiescent region. Perturbations transmitted in the gas phase cause the gas to move. Under the influence of the gas, the particles begin to accelerate and, after a certain amount of time, attain equilibrium with the gas phase with regard to velocity and temperature. Similarly to the relaxation zone in a frozen SW, the rarefaction wave propagating in the mixture is also associated with a relaxation zone. In the case described above, the relaxation zone is adjacent to the leading edge of the RW $x = x_\ell(t)$, which is characterized by the fact that the flow parameters are variable just to the left of the edge and are constant just to the right (we are speaking of the flow before the RW interacts with the wall).

Figure 5 shows theoretical x–t diagrams of the propagation of the head of the RW in the HPC at $p_1/p_0 = 350$; 5) pure gas in the HPC, 2) gas suspension with $\eta = 50$, $d = 20$ μm, 3) gas suspension with $\eta = 50$, $d = 40$ μm. Here, the front of the RW in the calculation was determined from the position of the point at which the pressure of the gas differed 2% from the undisturbed pressure in the HPC. Such a criterion makes it possible to allow for the effect of artificial viscosity, which causes erosion of the front. Figure 5 also shows curve 1, corresponding to the trajectory of the head of the RW obtained from the equilibrium theory, $x = a_e t$, $a_e = 136$ m/sec. Curve 4 in Fig. 4 represents the trajectory of the head of the RW in a pure gas with $x = at$, $a = 1014$ m/sec. At the initial moment of time, the diaphragm was located in the cell $i = 100$. It follows from a comparison of analytical curve 4 and theoretical curve 5 that computational effects lead to overstatement of the velocity of the RW head at the initial moments of time. Analysis of the calculations permits the conclusion that the "apparent" velocity of the front edge of the RW can be determined in the gas suspension. This quantity can be fixed in the experiment. It is also possible to determine the actual velocity of the leading edge, which is attenuated considerably by processes related to interphase friction. Here, we can make an analogy with the general theory of propagation of perturbations in relaxing media [15], where the leading edge moves at the velocity a_f and rapidly decaying harmonics are formed. That part of the signal represented by slowly decaying harmonics moves at the velocity a_e, $a_f > a_e$. For a gas suspension, the "apparent" velocity of the RW head changes over time from a_f to a_e [16]. As can be seen from Fig. 5, the transition to the equilibrium sonic velocity occurs more rapidly with a reduction in particle diameter.

The decay of the leading edge of the perturbations from the RW can be illustrated by using the example of the problem of the decay of a discontinuity for the system of equations describing a gas flow in a tube with rigidly fixed particles in an acoustic approximation:

$$\rho_t + \rho_0 u_x = 0, \quad u_t + \frac{c_0^2}{\rho_0}\rho_x = -\alpha u, \quad \alpha > 0 \tag{1}$$

with the initial conditions $x > 0$, $\rho = \rho^+$, $u = 0$; $x \le 0$, $\rho = \rho^-$, $u = 0$, $\rho^+ > \rho^-$. It is assumed that the particles exert a force on the gas proportional to the velocity of the gas. At $C_D = 24/Re$, we obtain $\alpha \sim d^{-2}$. System (1) reduces to the well-known telegraph equation (without loss of generality, we can take $\rho_0 = 1$, $c_0 = 1$), which by means of the substitution $w = \exp(-\alpha t/2)$, $z = \alpha(x + t)/2$, $y = \alpha(x - t)/2$ in turn reduces to the form

$$w_{zy} + w/4 = 0. \tag{2}$$

Having used the solution of Eq. (2) found in [17] by Riemann's method, we can represent the solution of system (1) in the form

$$\rho(x, t) = \left[\frac{\alpha}{4}\int_{x-t}^{x+t}\rho_0(\lambda)\left(\frac{\alpha^2 t J_1(-\xi)}{8\xi} + J_0(-\xi)\right)d\lambda + (\rho_0(x-t) + \rho_0(x+t))/2\right]\exp(-\alpha t/2), \tag{3}$$

where $\xi = \alpha^2((x - \lambda)^2 - t^2)^{0.5}/4$; J_0, J_1 are zeroth- and first-order Bessel functions.

It follows from (3) that the amplitude of the discontinuity, propagating to the right (being the analog of the RW in the present case), changes in accordance with the law $[\rho] = 0.5(\rho^+ - \rho^-)\exp(-\alpha t/2)$.

Figure 6 shows results of calculations with Eq. (3) at $\rho^+ = 3$, $\rho^- = 1$ for the moment of time $t = 1$ with $\alpha = 25$, 4, and 0.04 (lines 1-3). It is evident that an increase in the coefficient α, corresponding to a reduction in particle diameter, leads to decay of the leading edge.

Thus, we numerically analyzed the wave pattern of flow which develops in the dispersion of a cloud of particles with an appreciable concentration of the disperse phase. Quantitative estimates were given for the attenuation of the shock wave which occurs in a pure gas with variation of the initial parameters of the mixture. We also determined the RW in the mixture and found its structure. It was shown that, in contrast to gas dynamics (equilibrium), the leading edge of the RW propagates at a variable velocity which changes from a_f to a_e during flow. A comparison with the available experimental results [4] permits the conclusion that the mathematical model adequately describes the phenomenon for appreciable concentrations.

We thank B. E. Gel'fand for his assistance in the investigation.

LITERATURE CITED

1. A. N. Kraiko, R. I. Nigmatulin, V. K. Starkov, and L. E. Sternin, "Mechanics of multiphase media," Itogi Nauki Tekh. Ser. Gidromekh., 6 (1972).
2. A. I. Ivandaev, A. G. Kutushev, and R. I. Nigmatulin, "Gas dynamics of multiphase media. Shock and detonation waves in gas suspensions," Itogi Nauki Tekh. Ser. Mekh. Zhidk. Gaza, 16 (1981).
3. N. N. Yanenko, R. I. Soloukhin, A. N. Papyrin, and V. M. Fomin, Supersonic Two-Phase Flows under Conditions of Particle Velocity Nonequilibrium [in Russian], Novosibirsk, Nauka (1980).
4. B. E. Gel'fand, A. V. Gubanov, et al., "Shock waves in the dispersion of a compressed volume of a gas suspension of solid particles," Dokl. Akad. Nauk, SSSR, 281, No. 5 (1985).
5. G. Rudinger and A. Chang, "Analysis of nonsteady two-phase flow," Phys. Fluids, 7, No. 11 (1964).

6. A. I. Ivandaev, A. G. Kutushev, and R. I. Nigmatulin, "Numerical study of the dispersion of a cloud of finely dispersed particles or droplets by an explosion," Izv. Akad. Nauk SSSR Mekh. Zhidk. Gaza, No. 1, (1982).
7. A. V. Fedorov, "Analysis of equations describing a coal and gas outburst," Chisl. Metody Mekh. Sploshn. Sredy, 11, No. 4 (1980).
8. Yu. V. Kazakov, A. V. Fedorov, and V. M. Fomin, Structures of Isothermal Shock Waves and Calculation of the Dispersion of a Cloud of Particles [in Russian], Preprint, ITPM SO AN SSSR, No. 8 (1986).
9. A. I. Ivandaev, "Flow in a shock tube in the presence of suspended particles," Fiz. Goreniya Vzryva, No. 3 (1984).
10. I. Sh. Akhatov and P. B. Vainshtein, "Nonsteady regimes of combustion of porous propellants," Fiz. Goreniya Vzryva, No. 3 (1983).
11. O. M. Belotserkovskii and Yu. M. Davydov, Coarse Particle Method in Gas Dynamics. Computational Experiment [in Russian], Nauka, Moscow (1982).
12. Yu. V. Kazakov, S. P. Kiselev, A. V. Fedorov, and V. M. Fomin, "Propagation of discontinuities in mixtures," Summary of Documents of the All-Union Seminar "Current Problems and Mathematical Methods in the Theory of Filtration," Moscow (1984).
13. H. B. Stewart and B. Wendroff, "Two-phase flows: models and methods," J. Comput. Phys., 56, No. 3 (1984).
14. A. P. Ershov, "On the equations of the mechanics of two-phase media," Zh. Prikl. Mekh. Tekh. Fiz., No. 6 (1983).
15. J. Clark and M. McChesney, Dynamics of Real Gases [Russian translation], Mir, Moscow (1967).
16. Yu. V. Kazakov, A. V. Fedorov, and V. M. Fomin, "Analysis of the propagation of weak disturbances in gas suspensions," in: Numerical Methods of Solving Problems of the Theory of Elasticity and Plasticity, ITPM SO AN SSSR, Novosibirsk (1986).
17. R. Courant, Equations in Partial Derivatives [Russian translation], Mir, Moscow (1964).

CANONICAL TENSOR IN THE THEORY OF ELASTICITY

V. V. Kuznetsov

UDC 539.3

The study [1] presented a noncanonical form of a symmetrical tensor whereby the tensor assumes the simplest possible (diagonal) form in principal axes. Here, we define a symmetrical tensor which changes the quadratic form of the potential energy in a unit volume of an elastic body to canonical form. It is shown that such a transformation can be made by an appropriate selection of two constants in a form analogous to the generalized Hooke's law.

The stress–strain state in an elementary volume of an elastic body is characterized by the stress tensor σ_{ij} and the strain tensor ε_{ij} (i, j = 1, ..., 3). The components of these tensors are connected by the elasticity relations

$$\sigma_{ij} = b_{ijkm}\varepsilon_{km}. \tag{1}$$

Here and below, b_{ijkm} is the tensor of the elastic constants. Summation is carried out over twice-repeated subscripts. In an isotropic elastic body

$$b_{ijkm} = \lambda\delta_{ij}\delta_{km} + \mu(\delta_{ik}\delta_{jm} + \delta_{im}\delta_{jk}), \tag{2}$$

where λ and μ are the Lamé constants; δ_{ij} is the Kronecker symbol.

We will define the canonical tensor s_{ij} as a tensor having components connected with the components of the strain tensor by the same relations that connect the components of the stress tensor with the components of the canonical tensor, i.e.,

$$s_{ij} = c_{ijkm}\varepsilon_{km}; \tag{3}$$

Novosibirsk. Translated from Zhurnal Prikladnoi Mekhaniki i Tekhnicheskoi Fiziki, No. 5, pp. 144-146, September-October, 1987. Original article submitted June 26, 1986.

 0021-8944/87/2805- 0778 $12.50